



Alkali promoted the adsorption of toluene by adjusting the surface properties of lignin-derived carbon fibers

Min Song¹ · Lei Yu¹ · Bing Song¹ · Fanyue Meng¹ · Xinhong Tang¹

Received: 3 February 2019 / Accepted: 14 May 2019 / Published online: 31 May 2019
© Springer-Verlag GmbH Germany, part of Springer Nature 2019

Abstract

The lignin-based carbon fibers were prepared by electrospinning followed by stabilization, carbonization, and activation (i.e., steam activation, one-step KOH activation, and metal activation). The effect of carbonization temperature on prepared carbon fibers (CFs) was investigated. As a result, 800 °C is the most suitable carbonization temperature because the prepared carbon fibers possess greater specific surface area and pore volume. With the help of various characterization methods, the structural characteristics of the activated carbon fibers (ACFs) prepared by the three activation methods and the adsorption performance of toluene were compared. It was observed that the activated carbon fibers prepared by KOH one-step activation method (ACFK) exhibited higher specific surface area (1147.16 m²/g) and greater toluene adsorption (463 mg/g). Particularly, abundant microporous structures and surface functional groups play a vital role in the adsorption process. Further, the adsorption performance of toluene onto ACFK was further investigated in a gas-phase dynamic adsorption system and the results showed that ACFK has great potential application in adsorption of volatile organic compounds.

Keywords Lignin · Activated carbon fibers · Electrospinning · Activation · Volatile organic compounds

Introduction

As a new type of pollutant, volatile organic compounds (VOCs) in air, such as benzene, toluene, methanol, acetone, and formaldehyde, have been paid more and more attention in recent years for its wide distribution (Davardoost and Kahforoushan 2018; Nar et al. 2016). VOCs, which widely

exist in the atmosphere and water body, have a great harm on the environment and human beings (Chen et al. 2015; Shamskar et al. 2019). Therefore, the purification of VOCs in the environment needs to be effectively solved. At present, the researchers have carried out much research on the removal of VOCs (Aboukaïs et al. 2016; Song et al. 2017). Among the commonly used removal methods of VOCs, adsorption is the most effective, simple, and economical method (Wang et al. 2018; Yu et al. 2015).

For the adsorption method, a highly efficient and cheap adsorbent is the main problem faced by the researchers. Carbonaceous materials especially for the activated carbon (AC) have been extremely successful as an excellent alternative for VOC removal due to their big surface area, high adsorption capacity, and great reproducibility of the materials (Yuan et al. 2011; Laskar et al. 2018). Pak et al. applied activated carbon modified with sulfuric acid to enhance mixed VOC removal, and the adsorption amount of toluene on modified AC was increased by 18% compared with that on the commercial AC (Pak et al. 2016). Li et al. used rice husk-based activated carbon to remove VOCs by adsorption under various humidity conditions, which proved that the chemical functional groups on the surface of AC facilitate the attraction of hydrophilic VOCs (Li et al. 2016). Compared with AC, a

Responsible editor: Philippe Garrigues

✉ Min Song
minsong@seu.edu.cn

Lei Yu
yulei621627@126.com

Bing Song
2510916658@qq.com

Fanyue Meng
mfyseuer@163.com

Xinhong Tang
747338318@qq.com

¹ Ministry of Education of Key Laboratory of Energy Thermal Conversion and Control, School of Energy and Environment, Southeast University, Nanjing 210096, China

fibrillary shape makes activated carbon fibers (ACFs) have faster intraparticle adsorption kinetics than the granular activated carbons. Due to these advantages, some researchers applied ACFs into the removal of VOCs. Ju et al. prepared the activated carbon nanofibers by electrospinning of a polyacrylonitrile–cellulose acetate blending solution, which showed great adsorption behavior of toluene (Ju and Oh 2017). Baur et al. prepared the ACFs using phenolic precursor fibers and applied them into the removal of acetaldehyde, which also exhibited great adsorption performance (Baur et al. 2015). However, the common raw materials utilized in the synthesis of carbon fibers (CFs) are viscose, fossil pitch, and polyacrylonitrile (Nthumbi and Ngila 2016), which are nonrenewable and high priced. It is worth noting that lignin as a renewable source is the second abundant natural polymer after cellulose in nature (Nar et al. 2016). The high availability of lignin has sparked interest on its utilization as a precursor of carbon fibers (Wang et al. 2014).

In the manufacturing process of ACFs, the overall preparation steps are as followed: fiber spinning, thermostabilization, carbonization, and activation (Li et al. 2011; Streckova et al. 2016). And the purpose of stabilization is to make the spun fibers infusible. The carbonization is to consolidate their carbonaceous structure in order to get the CFs, while the activation is to obtain the ACFs. Up to date, ACFs are prepared by the chemical or physical activation of CFs. The related research about these four consecutive steps has been reported. Braun et al. investigated the effect of stabilization using the thermostabilization of lignin fibers as precursors for carbon fibers up to 340 °C at various heating rates in air (Braun et al. 2005). Ruiz-Rosas et al. prepared the submicron-diameter carbon fibers by the electrospinning with lignin, which illustrated the effect of the carbonization temperature (Ruiz-Rosas et al. 2010). Díez et al. proposed a novel approach to produce the chemically activated carbon fibers (Díez et al. 2015). Though much research has been conducted, it is not enough. The effects of different preparation methods on the adsorption performance of lignin-based activated electrospun carbon fibers have not been illustrated clearly.

In this study, a series of lignin-derived activated carbon fibers (ACFs) were prepared by electrospinning, thermostabilization, carbonization, and different activation methods. Additionally, the effects of various carbonization temperatures on the structural properties of the prepared activated carbon fibers were investigated. After batch experiments, the suitable activation method and temperature were finally screened out. Further, to better reveal the adsorption performance of as-prepared CFs or ACFs, the toluene in gas phase as a representative VOC was selected to present the adsorption properties of products.

Materials and methods

Chemicals and reagents

Lignin alkali, poly(vinyl alcohol) (PVA), acetic acid, ferric nitrate ($\text{Fe}(\text{NO}_3)_3 \cdot 9\text{H}_2\text{O}$), nickel nitrate ($\text{Ni}(\text{NO}_3)_2 \cdot 6\text{H}_2\text{O}$), zinc nitrate ($\text{Zn}(\text{NO}_3)_2 \cdot 6\text{H}_2\text{O}$), and potassium hydroxide (KOH) were purchased from the Sinopharm Chemical Reagent Co. Ltd. (Shanghai, China) and used to prepare various activated carbon fibers. Toluene was purchased from Lingfeng Chemical Reagent Co. Ltd. (Shanghai, China). All chemical reagents were of analytical-grade purity.

Fabrication of various lignin-derived activated carbon fibers

A series of lignin-derived activated carbon fibers (ACFs) were synthesized using electrospinning, thermostabilization, carbonization, and different activation methods. During the electrospinning process, the alkaline lignin was used as the precursor of fibers. The industrial analysis and elemental analysis for alkaline lignin was shown in Table 1. And the acetic acid was used as solvent to dissolve the lignin. In order to avoid the lignin aggregation in spinning solution, the 10 wt% polyvinyl alcohol (PVA) aqueous solution was selected as the dispersant (Ago et al. 2012). Lignin, PVA solution, and acetic acid were mixed according to the ratio of 1:1:3 (w/v/v), and the mixture solution was stirred at 80 °C for 30 min. The detailed electrospinning process can be referred to our previous work (Song et al. 2013). Then, the lignin-based fibers (LFs) were synthesized by an electrospinning machine (TL-OMNI, China). The prepared LFs could be applied to produce the CFs or ACFs followed by thermostabilities, carbonization, and activation.

Before carbonization and activation of LFs, stabilization is necessary. Stabilization was carried out under an air atmosphere. At this stage, the moisture and acetic acid components on the original fiber surface volatilize and the surface of the fiber was oxidized, which can prevent melting and cross-linking during subsequent carbonization step (Ruiz-Rosas et al. 2010; Díez et al. 2015). The alkaline lignin fibers were thermostabilized in a horizontal tubular furnace under air atmosphere whose flow rate was set as 150 mL/min. Then, the furnace was heated up to 200 °C and kept for 3 h.

The LFs after stabilization were subsequently carbonized and activated. Three different activation methods (i.e., steam physical, KOH chemical, and metal ion-catalyzed carbonization) were applied to activate LFs in this study. For the steam physical activation method, the thermostabilized LFs were subsequently carbonized at different temperatures (600–1000 °C, intervals 100 °C) to consolidate the carbonaceous structure of fibers under nitrogen atmosphere of 150 mL/min, and the carbonization time was 1 h. The physical

Table 1 Industrial analysis and elemental analysis of alkaline lignin

Samples	Elemental analysis/%					Industrial analysis/%			
	Cad	Had	Nad	Oad	Sad	Vad	FCad	Ad	Mad
Alkaline lignin	55.23	3.391	1.30	39.604	0.475	50.94	15.74	8.99	24.33

ad air dried basis, *d* dried basis

activation was subsequently conducted when the carbonation stage was done. The activation temperature increased to 800 °C and maintained for 30 min. The steam added into the tubular furnace was produced by the water flow of 5 mL/h heated with electric heating belt.

For the KOH activation method, the carbonization and activation steps were combined (Song et al. 2013). Different with conventional modification of carbon fibers by chemical activation method, the LFs after stabilization were thoroughly mixed with KOH powder particles at the weight ratio of 1:3 followed by carbonization treatment as above and the as-prepared activated carbon fiber was denoted as ACFK.

For the metallic activation method, however, the metal nitrates (i.e., nickel nitrate, zinc nitrate, and ferric nitrate) were added into the spinning solution whose metal mass fraction is 1%. And the lignin fibers containing metal were thermostabilized as well as carbonized. ACFZ, ACFN and ACFM respectively represent carbon fibers activated by metal activation method using ferric nitrate, zinc nitrate, and nickel nitrate as activation agents; ACFS and ACFK respectively refer to carbon fibers obtained by steam and KOH activation methods. The preparation process is shown in Fig. 1.

Characterization

In order to investigate the changes in the surface groups during the preparation of various fibers, the samples were characterized by Fourier infrared spectrometer (Nicolet iS10, Thermo Scientific, America). The porous textural parameters of prepared fibers were characterized by a specific surface area and pore size analyzer (ASAP 2020M, America). The surface morphology was studied by SEM (S-3000N, Hitachi, Japan)

and TEM (JEM-2100, JEOL, Japan). Additionally, Boehm titration was used to quantify the chemical functional groups on the surface of the as-prepared carbon materials.

The static and dynamic adsorption experiments

In order to better evaluate the adsorption performance of the prepared activated carbon fibers, static adsorption and dynamic adsorption experiments were carried out in this study. For the static adsorption, the prepared ACFs were put into the static adsorption bottle. Then, toluene was added into the bottle subsequent volatilization to simulate an environment with gaseous toluene of different concentrations. The temperature inside the bottle was changed by heating in a water bath. The static adsorption time was 2 h. The adsorption capacity q_e in static adsorption experiments is defined as follows:

$$q_e = \frac{m_1 - m_0}{m_0} \times 1000 \quad (1)$$

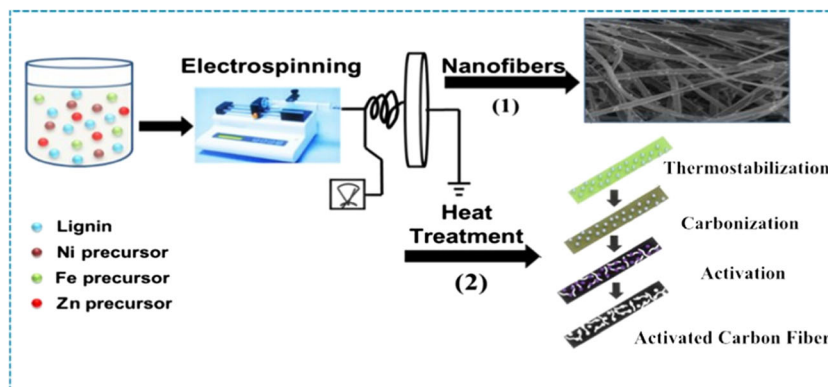
where q_e is the adsorption capacity (mg/g); m_0 and m_1 are the adsorbent weights before and after adsorption (g).

The dynamic adsorption experiment was conducted with a fixed bed reactor. The dynamic adsorption capacity and adsorption efficiency were calculated according to the following formula (Meng et al. 2019):

$$q_e = \frac{Q \int_0^t (C_{in} - C_{out}) dt}{m} \quad (2)$$

$$\eta = \frac{10^3 m q_e}{C_{in} t Q} \quad (3)$$

Fig. 1 The preparation process of lignin-based activated carbon fibers



In Eq. (2), q_e represents the adsorption capacity (mg/g); Q is the gas flow rate (L/min); C_{in} is the inlet concentration of toluene (mg/m³); C_{out} represents outlet concentration of toluene (mg/m³); m is the dosage of the adsorbent (g). In Eq. (3), η is the adsorption efficiency of the adsorbent for toluene (%); t represents the adsorption time (min).

Results and discussion

FTIR analysis

The preparation process of lignin-based carbon fibers is accompanied with complex physical and chemical changes, especially the fiber surface groups. Figure 2 represents the FTIR spectra of different fibers during the preparation processes of lignin-derived activated carbon fibers. As seen, the four kinds of materials all have complex absorption peaks. Some similar characteristic peaks could be observed in the spectra. For all four materials, the tensile vibration band of O–H at about 3396 cm⁻¹ was attributed to isolated O–H moieties and/or O–H in alcohol substance (Stobinski et al. 2010). There is a strong absorption peak at the band of 1550 cm⁻¹ of the four materials, which attributes to the C=C or C=O stretching vibration in aromatic. The band at 1205 cm⁻¹ is attributed to the O–H bending vibration in COOH groups or phenolic (Szabó et al. 2006). The obvious absorption peak at 588 cm⁻¹ could be attributed to the stretching vibration of C–C in aliphatic.

However, some of the stronger peaks can be observed in the FTIR spectrum. For lignin, LFs, and stabilized LFs, the bands at 2933 cm⁻¹ and 1135 cm⁻¹ correspond to the asymmetric stretching vibration bands of –CH₃ in the aromatic and symmetric stretching vibrational bands =C–H in the aromatic ring, respectively (Serna-Guerrero and

Sayari 2007); While for the CFs, these two functional groups disappeared due to high-temperature carbonization. Further, the band of the lignin spectrum at 1428 cm⁻¹ is the stretching vibration of –CH₃O (Huang et al. 2015). These results indicated that the oxygen-containing groups were introduced into CFs by thermo-stabilities and carbonization.

The effect of carbonization temperature

The effect of different carbonization temperatures (600, 700, 800, 900, 1000 °C) on the structural properties of the prepared activated carbon fibers is illustrated in Table 2. As shown, the yield of CFs decreases gradually with the increase of the temperature in the carbonization process. It is mainly due to the fact that the higher the temperature, the more complete the pyrolysis of lignin is, which leads to the decomposition of the molecule. And the bulk carbon of LFs may form a few graphitization structures, which also result in the yield decrease with the increase of temperature. This corresponds with the research from Keiluweit et al. (Keiluweit et al. 2010). With the increase of temperature, the microstructure is opened and well developed on the surface of the fibers, which leads to the specific surface area and pore structure of lignin-based CFs being optimized. When the temperature rises to 800 °C, the specific surface area and total pore volume reach the maximum values, which are 554.90 m²/g and 0.363 cm³/g respectively. However, when the temperature exceeds 800 °C, some of the pore structure on the surface of the carbon fiber collapses, which results in a decrease of the specific surface area and pore volume.

The prepared CFs with different specific surface areas were applied to the static adsorption of toluene to evaluate the adsorbent performance. As Table 2 showed, the trend of static adsorption capacity of toluene corresponds with specific surface area and total pore volume at different temperatures. When the carbonization temperature is

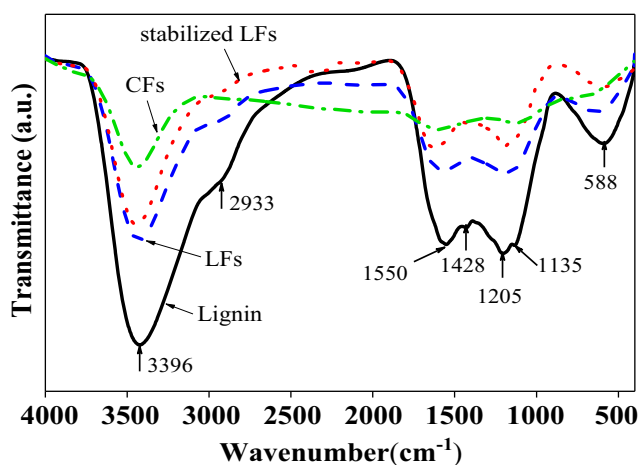


Fig. 2 FTIR spectra of the lignin-based CFs during the preparation processes

Table 2 Yield, S_{BET} , V_t , and q_e of carbon fibers at different temperatures

Temperature(°C)	Carbonization				
	600	700	800	900	1000
Yield (%)	35.5	34.8	31.1	28.2	25.9
S_{BET} (m ² /g)	431	509	555	441	408
V_t (cm ³ /g)	0.341	0.342	0.363	0.308	0.324
q_e (mg/g)	212.9	219.2	234.9	200.5	201.5

S_{BET} BET specific surface area, V_t total pore volume, q_e equilibrium adsorption capacity

Table 3 Elements analysis of ACFs

Samples	C (%)	H (%)	N (%)	S (%)	O (%)	O/C	N/C	H/C
ACFS	73.71	4.81	0.40	0.44	20.64	0.2800	0.0054	0.0653
ACFK	72.06	8.26	0.51	0.62	18.55	0.2575	0.0071	0.1071
ACFF	67.08	3.65	1.54	0.57	27.16	0.4049	0.0230	0.0544
ACFZ	67.09	3.05	0.31	0.55	29.00	0.4322	0.0046	0.0454
ACFN	64.26	4.26	0.08	0.57	30.83	0.4798	0.0012	0.0663

Table 4 ACF surface groups by Boehm titration

Samples	Carboxyl group (mmol/g)	Lactones groups (mmol/g)	Phenol hydroxyl (mmol/g)	Total acid groups (mmol/g)
ACFS	0.2996	0.2121	1.982	2.4937
ACFK	0.1642	0.2253	1.331	1.7205
ACFF	0.3516	0.3156	1.698	2.3652
ACFZ	0.3312	0.3209	1.875	2.5271
ACFN	0.5278	0.2986	1.873	2.6994

Table 5 Pore structure characteristics and adsorption capacity of different kinds of activated carbon fibers

Samples	ACFS	ACFK	ACFF	ACFZ	ACFN
S_{BET} (m ² /g)	807.77	1147.16	736.63	787.71	478.23
V_t (cm ³ /g)	0.484	0.638	0.561	0.432	0.737
S_{mic} (m ² /g)	388.6	942.29	286.29	486.02	338.94
V_{mic} (m ³ /g)	0.17	0.499	0.13	0.222	0.157
q_e (mg/g)	303.2	463	279.3	315.2	290.9

S_{BET} BET specific surface area, V_t total pore volume, S_{mic} micropore specific surface area, V_{mic} micropore volume, q_e equilibrium adsorption capacity

800 °C, the as-prepared activated carbon fiber has the largest adsorption capacity for toluene, which is 234.9 mg/g. Based on the above analysis, 800 °C was selected as the carbonization temperature of LFs.

The effect of different activation methods

Surface chemical analysis

The ACFs prepared by three different activation methods were measured via elemental analysis and Boehm titration, and the results are shown in Tables 3 and 4. As seen, the ACFs obtained by the three different activation methods have certain differences in the content of each element and the number of acidic groups. The activated carbon fibers prepared by the metal catalytic carbonization activation method have a high oxygen content, and the amount of carbon is reversed. Additionally, the metal catalytic carbonization method is significantly more expensive to produce than the steam activation method due to the addition of metal ions and the temperature rise of the furnace. Compared with the other two activation methods, the activated carbon fibers obtained by KOH one-step activation method (ACFK) also contains certain

acidic groups but the total content of various groups is less than that of the other two activated methods.

Specific surface area and pore size analysis

To further illustrate the effect of different activation methods on the surface properties of ACFs, the pore structure and static adsorption of toluene results are shown in Table 5. According to Table 5, for the micropore specific surface area and micropore volume, the ACFK prepared by KOH activation was the best one and the ACFZ added with zinc ion was the secondary. It has the same trend for the adsorption performance of toluene. Further, it was observed that, though the specific surface area and total pore volume of ACFS were the second largest, the adsorption capacity of toluene was not of the same trend. There was a positive correlation between adsorption capacity of toluene and micropore surface area as well as micropore volume, which indicated that microporous property was the key factor to adsorption performance of adsorbent. Combined with the results of surface chemical analysis, the preparation cost of the metal catalytic carbonization activation method is significantly higher than that of the steam activation method. In addition, at room temperature (298 K), the adsorption capacity of toluene is smaller than that of the KOH one-step

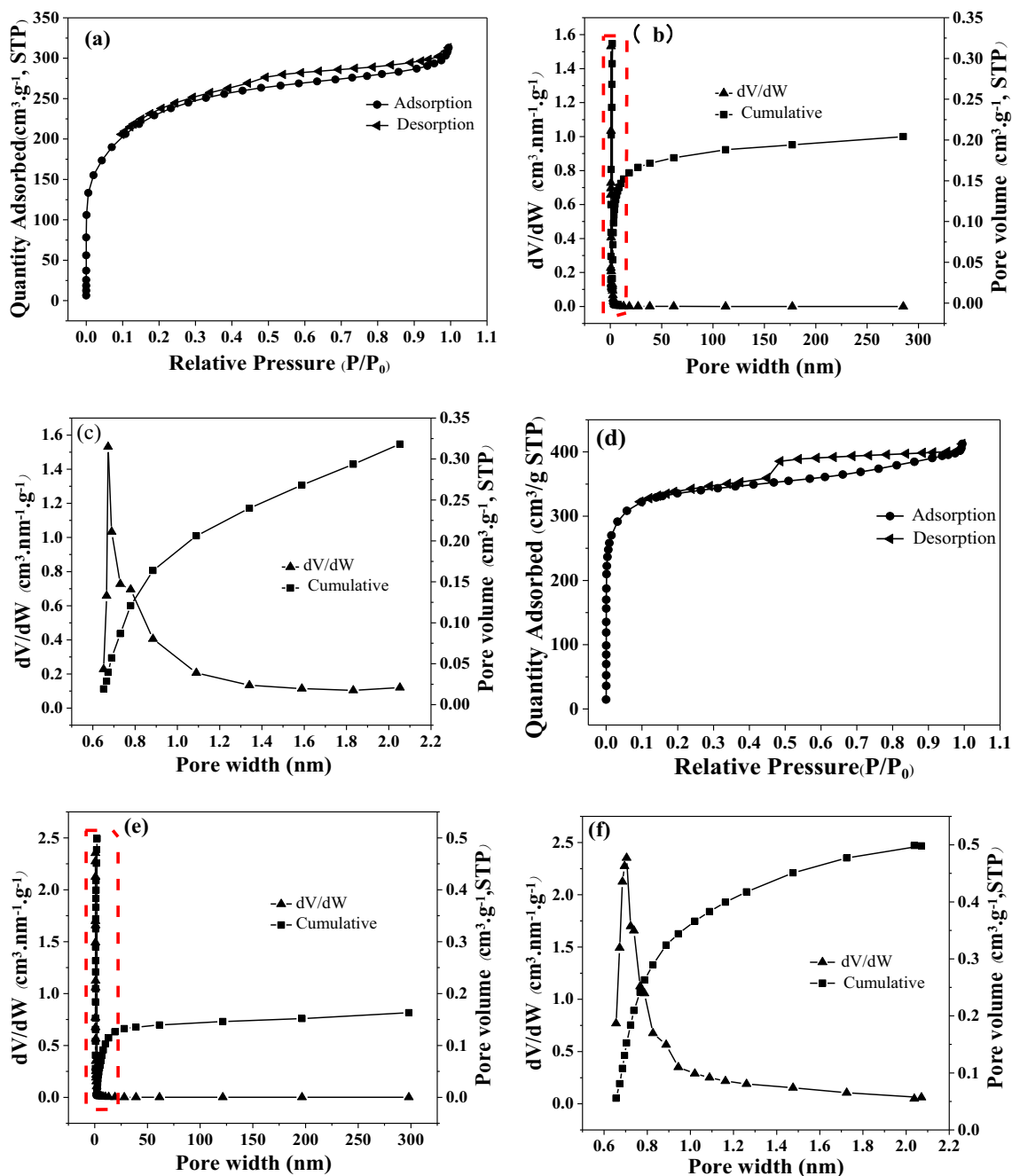


Fig. 3 N₂ adsorption-desorption isotherm at 77 K and pore size distribution of ACFS (a, c) and ACFK (c, d)

activation method. For comprehensive consideration, ACFS and ACFK were selected for further study.

The pore size distribution of the nitrogen adsorption-desorption isotherm of ACFS and ACFK was further analyzed, and the results are shown in Fig. 3. As seen in Fig. 3 (b) and (d), the pore size of ACFK is more concentrated in the part below 2 nm. Meanwhile, from the type of hysteresis loops in the N₂ adsorption-desorption isotherms in Fig. 3 (a) and (c), it can be concluded that the adsorption isotherms of ACFS and ACFK adsorbents for N₂ at 77.4 K belong to the type I isotherms of the five types of BDDT isotherms and the surface contains a

certain mesoporous structure, which is characterized by the adsorption process (Brunauer et al. 1940). When the relative pressure increases to a certain extent, the adsorption capacity increases sharply and there is no saturation phenomenon. Further, it can be seen from the size of the two hysteresis loops that the pore size of ACFK is mainly microporous.

Electron microscopy results

The morphologies of the as-prepared ACFS and ACFK were characterized by SEM and TEM images, and the

Fig. 4 SEM and TEM images of ACFS and ACFK

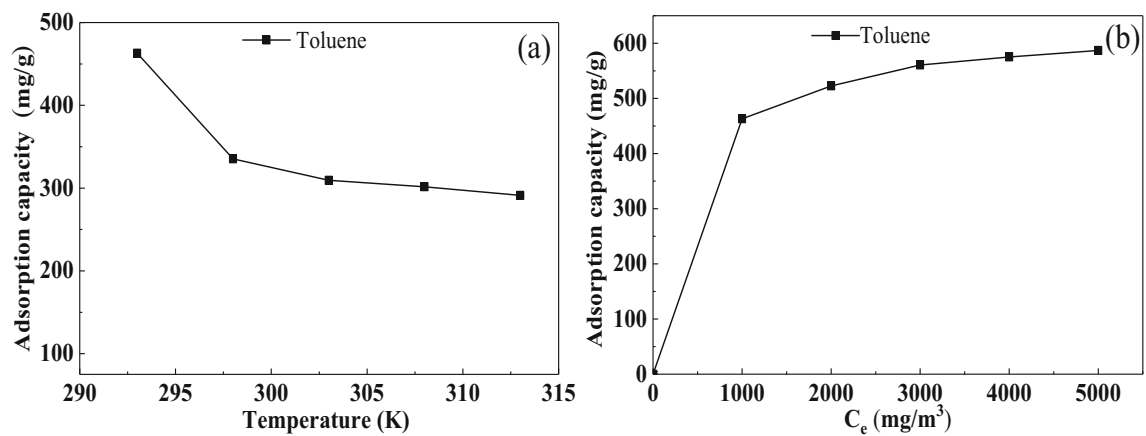
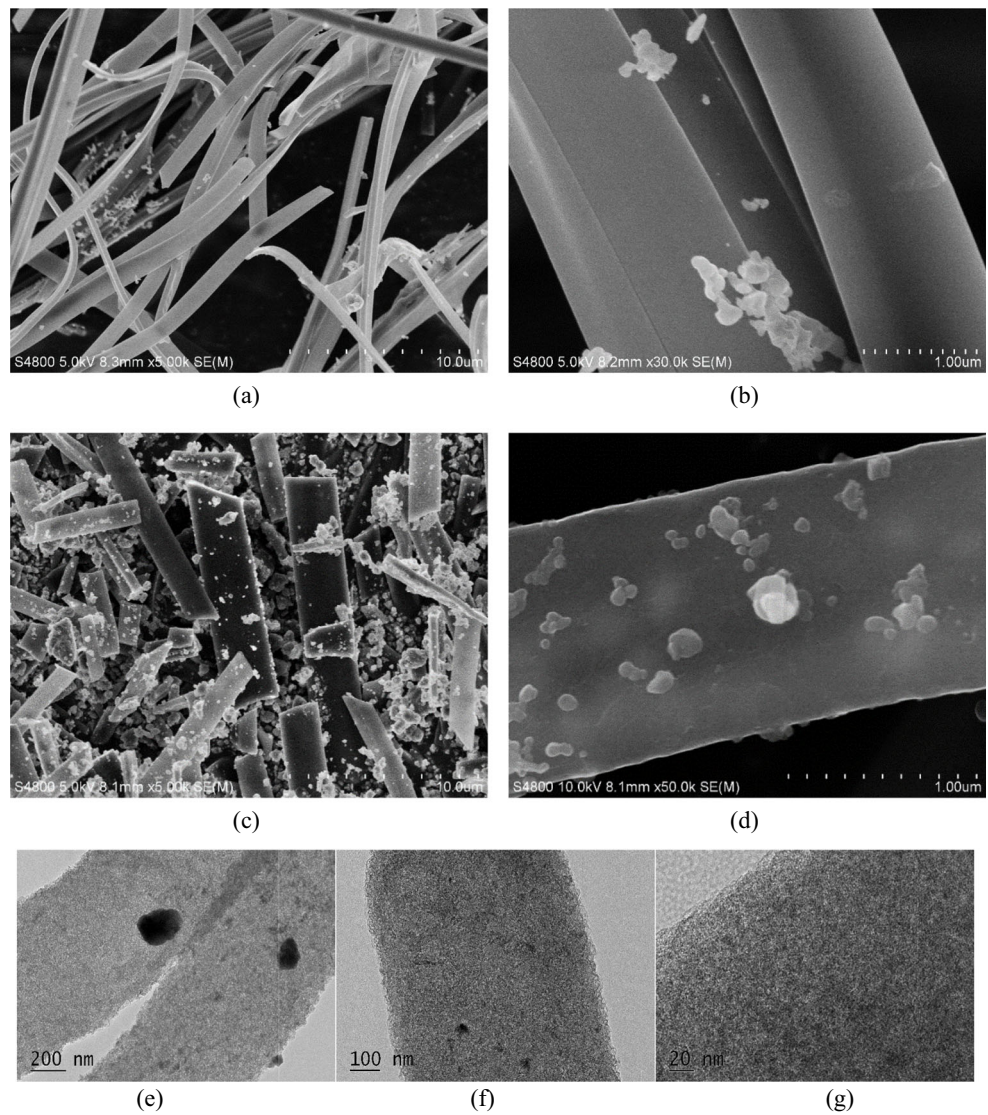


Fig. 5 Effects of temperature (a) and concentration of toluene (b) on the static adsorption capacity of ACFK. Conditions: the concentration of toluene is 1000 mg/m³, the dosage of adsorbent is 0.1 g, adsorption temperature 298 K, adsorption time 120 min

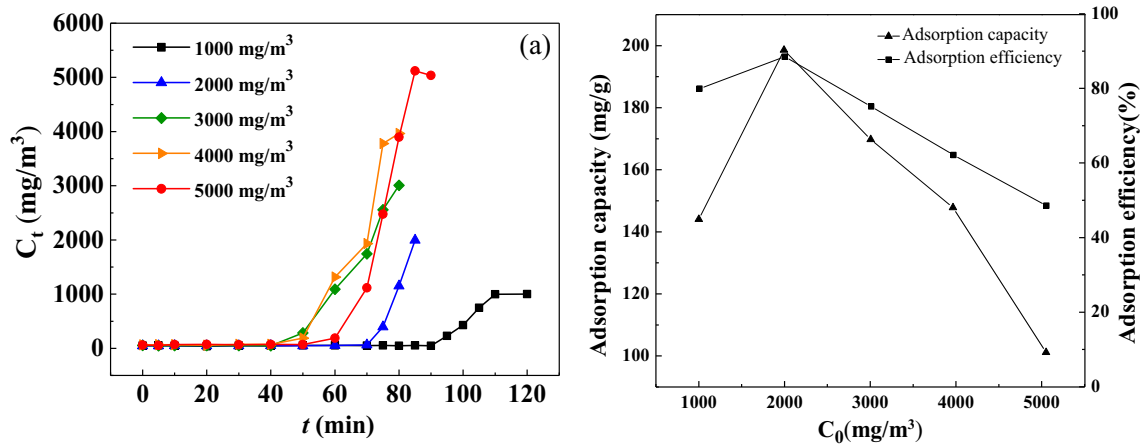


Fig. 6 Adsorption breakthrough curve (a) as well as the dynamic adsorption capacity and adsorption efficiency (b) of ACFK at different concentrations of toluene. Conditions: gas flow rate 150 mL/min, a balance of N₂, adsorption temperature 298 K

results are shown in Fig. 4. As shown, the ACFK prepared by KOH one-step activation method maintain the cylindrical structures. The surface of ACFK is rough and porous. Some small particles exist on the surface of ACFK because of the carbonization of residual acetic acid or PVA from spinning solution. Additionally, TEM image of ACFK presents that the fiber surface has obvious groove structure which may be the micropore below 2 nm. These characterization results fully illustrate the nature of the micropore for ACFK which correspond with the results of specific surface area and pore size analysis.

The adsorption performance of ACFK

Based on the above analysis, the ACFK prepared by one-step KOH activation was applied for the adsorption of toluene selected as the typical VOCs.

In the static adsorption system, the effects of temperature and equilibrium concentration (C_e) were investigated as shown in Fig. 5. In the case of ACFK, the equilibrium adsorption capacity (q_e) of toluene decreases with the increase of temperature. This is due to the fact that adsorption is an exothermic process, so the increase of temperature would cause a decrease in the adsorption capacity of toluene. According to the adsorption isotherm under 298 K as shown in Fig. 5 (b), it is the type I adsorption isotherm for adsorption of toluene which is attributed to the adsorption with micropore (Pei and Zhang 2012). The equilibrium adsorption capacity increases with the increase of concentration until the ACFs reach the maximum saturated adsorption capacity. On the one hand, the relatively high concentration increases the contact opportunity between adsorbate and adsorbent, which makes more toluene molecules adhere to ACFK surface. And

on the other hand, the adsorption capacity of toluene on the ACFK per unit volume is certain. When the concentration of toluene exceeds 3000 mg/m³, the adsorption capacity will not increase significantly.

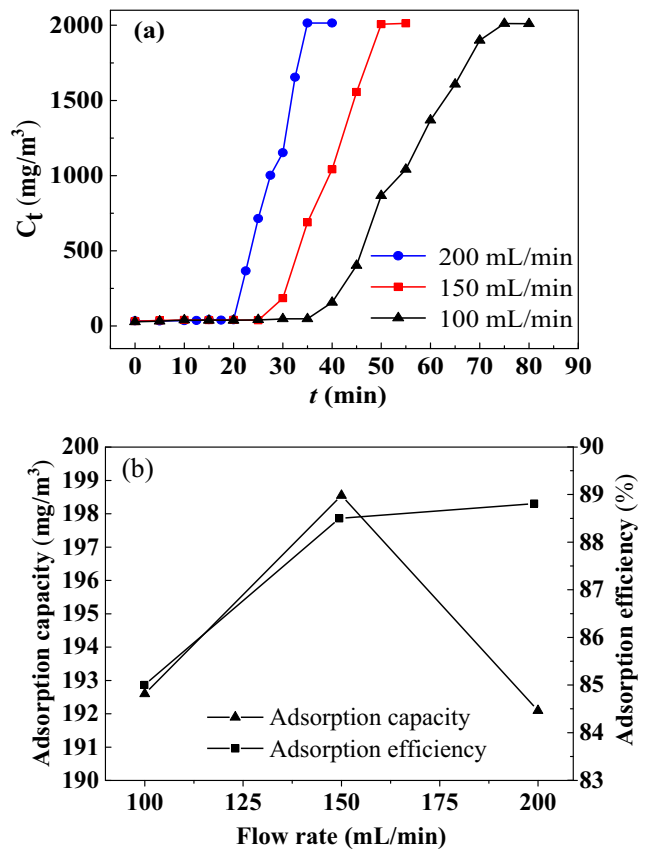


Fig. 7 Adsorption breakthrough curve (a) as well as the saturated adsorption capacity and adsorption efficiency (b) of ACFK at different flow rates. Conditions: a balance of N₂, adsorption temperature 298 K

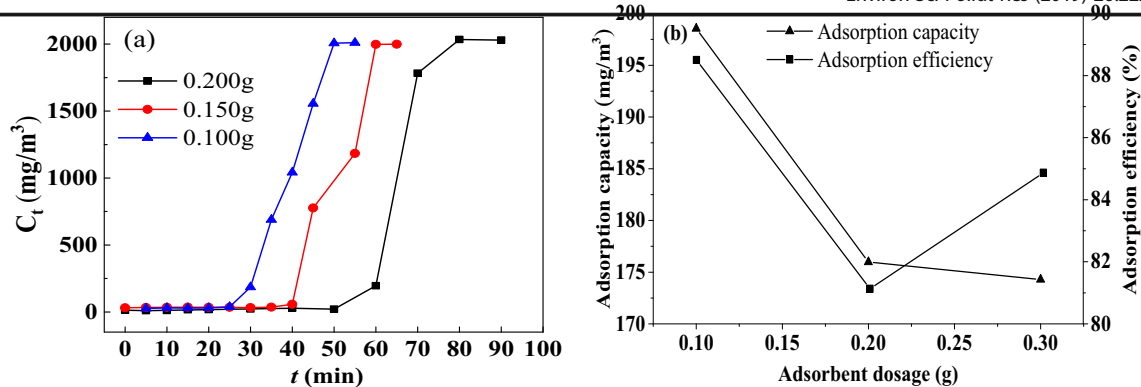


Fig. 8 Adsorption breakthrough curve (a) as well as the saturated adsorption capacity and adsorption efficiency of ACFK with different adsorbent dosages (b). Conditions: gas flow rate 150 mL/min, a balance of N₂, adsorption temperature 298 K

In order to better reveal the adsorption characteristics of the adsorbent, the dynamic adsorption experiments were conducted at different inlet concentrations of toluene, flow rates, and adsorbent dosages. The results about the outlet concentrations (C_t) and adsorption capacities are presented in Figs. 6, 7, and 8.

Figure 6 represents the adsorption breakthrough curves and the saturated adsorption capacities as well as adsorption efficiency at different inlet concentrations of toluene. The breakthrough curves of ACFK for toluene illustrate that the whole dynamic adsorption process consists of three stages (Zhao et al. 2018). Firstly, the toluene molecule is fully adsorbed by adsorbents. With the continuous inflow of toluene gas, adsorption enters into the second stage called initial breakthrough stage until the ACFs reach the maximum saturated adsorption capacity, which is the third stage called thorough breakthrough or saturated adsorption stage. As shown in Fig. 6 (a), with the increase of the inlet concentration of toluene, breakthrough points and saturated adsorption points moved left. With the help of the mathematical integral calculation, the adsorption capacities and adsorption efficiency of toluene onto the ACFK are shown in Fig. 6 (b). Both the adsorption capacities and adsorption efficiency increase first and then decrease with the increase of concentration of toluene. The biggest value is 198.55 mg/g and 88.5% respectively at the concentration of 2000 mg/m³.

The effect of flow rate on dynamic adsorption was conducted with a constant toluene inlet concentration of 2000 mg/m³ which is shown in Fig. 7. As shown in Fig. 7 (a), the higher flow rates, the shorter breakthrough time, and the steeper slope of the breakthrough curve mean a shorter time from the initial breakthrough stage to saturated adsorption. According to Fig. 7 (b), the saturated adsorption capacities increase first and then decrease while the adsorption efficiency increases continuously with the increase of concentration of toluene. The saturated adsorption capacity is 198.55 mg/g at the flow rate of 150 mL/min.

Keeping the flow rate of 150 mL/min and concentration of toluene 2000 mg/m³, the effect of adsorbent dosages on dynamic adsorption of toluene is shown in Fig. 8. When the adsorbent dosages increase from 0.1 to 0.3 g, the breakthrough curve moves right. Besides, the saturated adsorption capacities decrease first and then increase while the adsorption efficiency increases continuously with the increase of adsorbent dosages. Further, toluene as a typical component of VOCs has always been the focus of scholars' research. The dynamic adsorption data of toluene by carbon-based adsorbents are shown in Table 6. As seen, the saturated adsorption capacity of ACFK to toluene under dynamic conditions is slightly smaller than that of the two commercial carbon-based adsorbents (Zhang et al. 2010; Zhang et al. 2017) but still has obvious adsorption effect and excellent pore structure.

Table 6 Comparison of toluene adsorption by ACFK and commercial carbonaceous adsorbents

Adsorbents	S_{BET} (m ² /g)	V_t (cm ³ /g)	d (nm)	q_e (mg/g)
ACFK	1147	0.638	2.22	198.55
Viscose-based activated carbon fiber	1917	0.796	1.43	~400
Coconut shell-based activated carbon	1015	0.501	~2.10	~300

S_{BET} BET specific surface area, V_t total pore volume, d pore width, q_e equilibrium adsorption capacity

Conclusions

In this work, a series of alkaline lignin-based activated carbon fibers were prepared by KOH chemical and steam physical as well as metal activation methods. The surface properties of as-prepared materials were characterized via various analytical tools, and the results demonstrated a large number of micropores on the ACFK surface, which led to better adsorption performance than the steam and metal activation with respect to the porosity development. Furthermore, the as-prepared activated carbon fibers by means of KOH activation method exhibited a good adsorption performance in the static and dynamic adsorption of toluene, and the processes are rapid, efficient, and economic. All of these results demonstrated that lignin-derived activated carbon fibers activated by KOH have a potential application in adsorption of VOCs.

Funding information This work was supported by the National Key R&D Program of China (2018YFC1803100). The authors are grateful for Natural Science Foundation of Jiangsu Province (BK20181142).

References

- Aboukaïs A, Skaf M, Hany S, Cousin R, Aouad S, Labaki M, Abi-Aad E (2016) A comparative study of Cu, Ag and Au doped CeO₂ in the total oxidation of volatile organic compounds (VOCs). *Mater Chem Phys* 177:570–576. <https://doi.org/10.1016/j.matchemphys.2016.04.072>
- Ago M, Jakes JE, Johansson LS, Park S ROJ (2012) Interfacial properties of lignin-based electrospun nanofibers and films reinforced with cellulose nanocrystals. *ACS Appl Mater Interfaces* 4(12):6849–6856. <https://doi.org/10.1021/am302008p>
- Baur GB, Yuranov I, Kiwi-Minsker L (2015) Activated carbon fibers modified by metal oxide as effective structured adsorbents for acetaldehyde. *Catal Today* 249:252–258. <https://doi.org/10.1016/j.cattod.2014.11.021>
- Braun JL, Holtman KM, Kadla JF (2005) Lignin-based carbon fibers: oxidative thermo-stabilization of kraft lignin. *Carbon* 43(2):385–394. <https://doi.org/10.1016/j.carbon.2004.09.027>
- Brunauer S, Deming LS, Deming WE, Teller E (1940) On a theory of the van der Waals adsorption of gases. *J Am Chem Soc* 62(7):1723–1732. <https://doi.org/10.1021/ja01864a025>
- Chen XC, Luo Q, Wang DH, Gao JJ, Wei Z, Wang ZJ, Zhou HD, Mazumder A (2015) Simultaneous assessments of occurrence, ecological, human health, and organoleptic hazards for 77 VOCs in typical drinking water sources from 5 major river basins, China. *Environ Pollut* 206:64–72. <https://doi.org/10.1016/j.envpol.2015.06.027>
- Davardoost F, Kahforoushan D (2018) Health risk assessment of VOC emissions in laboratory rooms via a modeling approach. *Environ Sci Pollut Res* 25:17890–17900. <https://doi.org/10.1007/s11356-018-1982-6>
- Díez N, Álvarez P, Granda M, Blanco C, Santamaría R, Menéndez R (2015) A novel approach for the production of chemically activated carbon fibers. *Chem Eng J* 260:463–468. <https://doi.org/10.1016/j.cej.2014.08.104>
- Ju YW, Oh GY (2017) Behavior of toluene adsorption on activated carbon nanofibers prepared by electrospinning of a polyacrylonitrile-cellulose acetate blending solution. *Korean J Chem Eng* 34(10):2731–2737. <https://doi.org/10.1007/s11814-017-0171-5>
- Huang YX, Ma E, Zhao GJ (2015) Thermal and structure analysis on reaction mechanisms during the preparation of activated carbon fibers by KOH activation from liquefied wood-based fibers. *Ind Crop Prod* 69:447–455. <https://doi.org/10.1016/j.indcrop.2015.03.002>
- Keiluweit M, Nico PS, Johnson MG, Kleber M (2010) Dynamic molecular structure of plant biomass-derived black carbon (biochar). *Environ Sci Technol* 44(4):1247–1253. <https://doi.org/10.1021/es9031419>
- Laskar II, Hashisho Z, Phillips JH, Anderson JE, Nichols M (2018) Competitive adsorption equilibrium modeling of volatile organic compound (VOC) and water vapor onto activated carbon. *Sep Purif Technol* 212:632–640. <https://doi.org/10.1016/j.seppur.2018.11.073>
- Li L, Liu S, Liu J (2011) Surface modification of coconut shell based activated carbon for the improvement of hydrophobic VOC removal. *J Hazard Mater* 192(2):683–690. <https://doi.org/10.1016/j.jhazmat.2011.05.069>
- Li MS, Wu SC, Peng YH, Shih YH (2016) Adsorption of volatile organic vapors by activated carbon derived from rice husk under various humidity conditions and its statistical evaluation by linear solvation energy relationships. *Sep Purif Technol* 170:102–108. <https://doi.org/10.1016/j.seppur.2016.06.029>
- Meng FY, Song M, Wei YX, Wang YL (2019) The contribution of oxygen-containing functional groups to the gas-phase adsorption of volatile organic compounds with different polarities onto lignin-derived activated carbon fibers. *Environ Sci Pollut Res* 26(7):7195–7204. <https://doi.org/10.1007/s11356-019-04190-6>
- Nar M, Rizvi HR, Dixon RA, Chen F, Kovalcik A, D'Souza N (2016) Superior plant based carbon fibers from electrospun poly-(caffeyl alcohol) lignin. *Carbon* 103:372–383. <https://doi.org/10.1016/j.carbon.2016.02.053>
- Nthumbi RM, Ngila JC (2016) Electrospun and functionalized PVDF/PAN nanocatalyst-loaded composite for dechlorination and photodegradation of pesticides in contaminated water. *Environ Sci Pollut Res* 23(20):20214–20231. <https://doi.org/10.1007/s11356-016-7136-9>
- Pak SH, Jeon MJ, Jeon YW (2016) Study of sulfuric acid treatment of activated carbon used to enhance mixed VOC removal. *Int Biodeterior Biodegradation* 113:195–200. <https://doi.org/10.1016/j.ibiod.2016.04.019>
- Pei J, Zhang JS (2012) Determination of adsorption isotherm and diffusion coefficient of toluene on activated carbon at low concentrations. *Build Environ* 48:66–76. <https://doi.org/10.1016/j.buildenv.2011.08.005>
- Ruiz-Rosas R, Bedia J, Lallave M, Loscertales IG, Barrero A, Rodríguez-Mirasol J, Cordero T (2010) The production of submicron diameter carbon fibers by the electrospinning of lignin. *Carbon* 48(3):696–705. <https://doi.org/10.1016/j.carbon.2009.10.014>
- Serna-Guerrero R, Sayari A (2007) Applications of pore-expanded mesoporous silica. 7. Adsorption of volatile organic compounds. *Environ Sci Technol* 41(13):4761–4766. <https://doi.org/10.1021/es0627996>
- Shamskar KR, Rashidi A, Azar PA, Yousefi M, Baniyaghoob S (2019) Synthesis of graphene by in situ catalytic chemical vapor deposition of reed as a carbon source for VOC adsorption. *Environ Sci Pollut Res* 26(4):3643–3650. <https://doi.org/10.1007/s11356-018-3799-8>
- Song M, Jin BS, Xiao R, Yang L, Wu YM, Zhong ZP, Huang YJ (2013) The comparison of two activation techniques to prepare activated

- carbon from corn cob. *Biomass Bioenergy* 48(1):250–256. <https://doi.org/10.1016/j.biombioe.2012.11.007>
- Song M, Zhang W, Chen YS, Luo J, Crittenden JC (2017) The preparation and performance of lignin-based activated carbon fiber adsorbents for treating gaseous streams. *Front Chem Sci Eng* 11(3):328–337. <https://doi.org/10.1007/s11705-017-1646-y>
- Stobinski L, Lesiak B, Kövér L, Tóth J, Biniak S, Trykowski G, Judek J (2010) Multiwall carbon nanotubes purification and oxidation by nitric acid studied by the FTIR and electron spectroscopy methods. *J Alloy Compd* 501(1):77–84. <https://doi.org/10.1016/j.jallcom.2010.04.032>
- Streckova M, Mudra E, Orinakova R, Markusova-Buckova L, Sebek M, Kovalcikova A, Sopcak T, Girman V, Dankova Z, Micusik M, Dusza J (2016) Nickel and nickel phosphide nanoparticles embedded in electrospun carbon fibers as favourable electrocatalysts for hydrogen evolution. *Chem Eng J* 303:167–181. <https://doi.org/10.1016/j.cej.2016.05.147>
- Szabó T, Berkesi O, Forgó P, Josepovits K, SanakisY PD, Dékány I (2006) Evolution of surface functional groups in a series of progressively oxidized graphite oxides. *Chem Mater* 18(11):2740–2749. <https://doi.org/10.1021/cm060258+>
- Wang SS, Zhang L, Long C, Li AM (2014) Enhanced adsorption and desorption of VOCs vapor on novel micro-mesoporous polymeric adsorbents. *J Colloid Interf Sci* 428:185–190. <https://doi.org/10.1016/j.jcis.2014.04.055>
- Wang D, Wu G, Zhao Y, Cui L, Shin CH, Ryu MH, Cai J (2018) Study on the copper(II)-doped MIL-101(Cr) and its performance in VOCs adsorption. *Environ Sci Pollut Res* 25(28):28109–28119. <https://doi.org/10.1007/s11356-018-2849-6>
- Yu XQ, Sun WL, Ni JR (2015) LSER model for organic compounds adsorption by single-walled carbon nanotubes: comparison with multi-walled carbon nanotubes and activated carbon. *Environ Pollut* 206:652–660. <https://doi.org/10.1016/j.envpol.2015.08.031>
- Yuan CG, Zhang Y, Wang S, Chang A (2011) Separation and preconcentration of palladium using modified multi-walled carbon nanotubes without chelating agent. *Microchim Acta* 173(3–4):361–367. <https://doi.org/10.1007/s00604-011-0565-8>
- Zhang TY, Yang QS, Shi HX, Han C, Liu X (2010) Adsorption of naphthalene on a viscose-based activated carbon fiber. *Acta Phys -Chim Sin* 26(2):367–372. <https://doi.org/10.3866/PKU.WHXB20100221>
- Zhang X, Gao B, Creamer AE, Cao CC, Li YC (2017) Adsorption of VOCs onto engineered carbon materials: a review. *J Hazard Mater* 338:102–123. <https://doi.org/10.1016/j.jhazmat.2017.05.013>
- Zhao X, Li X, Zhu T, Tang X (2018) Adsorption behavior of chloroform, carbon disulfide, and acetone on coconut shell-derived carbon: experimental investigation, simulation, and model study. *Environ Sci Pollut Res* 25(31):31219–31229. <https://doi.org/10.1007/s11356-018-3103-y>

Publisher's note Springer Nature remains neutral with regard to jurisdictional claims in published maps and institutional affiliations.